Neurochemical Research
https://doi.org/10.1007/s11064-022-03806-7

ORIGINAL PAPER

Munc18-1 Contributes to Hippocampal Injury in Septic Rats Through Regulation of Syntanxin1A and Synaptophysin and Glutamate Levels

Fajuan Tang[1,2] · Lin Chen[1] · Hu Gao[1,2] · Yupeng Lei[1,2] · Linli Pan[1,2] · Dongqiong Xiao[1,2] · Xihong Li[1,2]

Received: 1 July 2022 / Revised: 7 October 2022 / Accepted: 20 October 2022

Abstract

Sepsis-associated encephalopathy (SAE) is a diffuse brain dysfunction closely associated with mortality in the acute phase of sepsis. Abnormal neurotransmitters release, such as glutamate, plays a crucial role in the pathological mechanism of SAE. Munc18-1 is a key protein regulating neurotransmission. However, whether Munc18-1 plays a role in SAE by regulating glutamate transmission is still unclear. In this study, a septic rat model was established by the cecal ligation and perforation. We found an increase in the content of glutamate in the hippocampus of septic rat, the number of synaptic vesicles in the synaptic active area and the expression of the glutamate receptor NMDAR1. Meanwhile, it was found that the expressions of Munc18-1, Syntaxin1A and Synaptophysin increased, which are involved in neurotransmission. The expression levels of Syntaxin1A and Synaptophysin in hippocampus of septic rats decreased after interference using Munc18-1siRNA. We observed a decrease in the content of glutamate in the hippocampus of septic rats, the number of synaptic vesicles in the synaptic activity area and the expression of NMDAR1. Interestingly, it was also found that the down-regulation of Munc18-1 improved the vital signs of septic rats. This study shows that CLP induced the increased levels of glutamate in rat hippocampus, and Munc18-1 may participate in the process of hippocampal injury in septic rats by affecting the levels of glutamate via regulating Syntaxin1A and Synaptophysin. Munc18-1 may serve as a potential target for SAE therapy.

Keywords Munc18-1 · Neurotransmission · Glutamate · Sepsis-associated encephalopathy · Rats

Introduction

Sepsis is an organ dysfunction that is caused by an imbalanced response of the body to infection, and it has a high incidence and mortality rate [1]. The brain is the first affected organ during sepsis [2]. Sepsis-associated encephalopathy (SAE) is a diffuse brain dysfunction, mainly manifested as changes in consciousness and cognitive dysfunction [2]. The main parts of the brain affected by sepsis are the frontal cortex and hippocampus [3]. The latter plays a key role in the process of learning and memory [4]. SAE increases the mortality of sepsis in the acute phase, and causes cognitive dysfunction and loss of attention, memory and executive ability in the long-term [5, 6]. The pathogenesis of SAE is still unclear. It is considered that some processes including microglia activation, blood-brain barrier destruction, hypoxia, neurotransmitter imbalance, axon and neuron loss are involved [7, 8]. There is no effective treatment for SAE-associated cognitive dysfunction so far. Therefore, more basic research should be performed to understand the pathological process of SAE and explore new therapeutic targets.

✉ Dongqiong Xiao
m13881749494@163.com

✉ Xihong Li
lixihonghxey@163.com

Fajuan Tang
kftangfajuan@163.com

Lin Chen
lcychenlin@163.com

Hu Gao
drgaohu@163.com

Yupeng Lei
leiyupenghxey@163.com

Linli Pan
Panlingli1980@163.com

[1] Department of emergency, West China Second University Hospital, Sichuan University, Chengdu, Sichuan 610041, China

[2] Key Laboratory of Birth Defects and Related Diseases of Women and Children (Sichuan University), Ministry of Education, Chengdu 610041, China

Published online: 05 November 2022

Glutamate represents the main excitatory neurotransmitter in the brain. During sepsis, the release of glutamate increases and its reuptake decreases [9, 10]. N-methyl-D-aspartate receptor (NMDAR) is mainly located in the postsynaptic membrane and consists of 3 subunits, NMDAR1, NMDAR2 and NMDAR3 [11]. NMDAR1 is the main functional subunit and has all the properties of the NMDARs channel complex [11]. NMDARs belong to a family of ligand-gated ion channels and are closely related to synaptic plasticity as well as learning and memory, and there are two glutamate binding sites on each NMDAR [11]. Excessive glutamate activates the NMDAR, which produces excitotoxicity to cause nerve cell degeneration [12]. The transmission of the neurotransmitter depends on the fusion of synaptic vesicles with the plasma membrane, a process which is regulated by a variety of proteins [13]. The soluble N-ethylmaleimide-sensitive factor attachment protein receptors (SNARE) is a presynaptic membrane regulatory protein, which is composed of Synaptobrevin, Syntaxin1 and Synaptosomal-associated protein of 25kD (SNAP-25) [14]. Syntaxin1 is the core protein of SNARE, and mainly has two subtypes: Syntaxin1A and Syntaxin1B[14]. Syntaxin1A mainly mediates the docking and fusion of synaptic vesicles in the synaptic active area, and its expression level reflects the number of synaptic vesicles in the synaptic active area at a certain extent [14]. Munc18-1 (encoded by the *STXBP1* gene) is a synaptic fusion protein binding protein, which interacts with Syntaxin1A to regulate synaptic vesicle anchoring and fusion to affect the neurotransmitter transmission [15]. A previous study has found that the decreased expression of Munc18-1 affects the number of released synaptic vesicles and supply of vesicles, which in turn affects the transmission of neurotransmitters, such as glutamate and gamma-aminobutyric acid (GABA), which impairs learning and memory [16]. Synaptophysin is a key synaptic vesicle protein that can correctly target the synaptic vesicles to the presynaptic membrane by regulating Synaptobrevin-II [17]. In addition, it plays an important role in the membrane transport, docking and fusion of synaptic vesicles [18].

Munc18-1 had been studied in various neurological diseases, including schizophrenia and autism [19, 20]. However, its role in SAE has not been investigated. In this study, a rat model of sepsis was established by cecal ligation and perforation (CLP), and the expression of Munc18-1 in the hippocampus of septic rats was investigated. Meanwhile, this study further explored the possible mechanism of Munc18-1 involvement in SAE.

Materials and Methods

Animals

Thirty-day-old clean and healthy male Sprague-Dawley rats (SD) rats (with the age equivalent to human 2–11 year [21, 22] and weight between 100 and 120 g) were purchased from Sichuan Jianyang Dashuo Animal Science and Technology Co., Ltd (Shu ICP 09003144). All the operations in this study are in lined with the Research Animal Care Committee of Sichuan University and all the experiments were performed in accordance with the guidelines. All the rats were housed in a 55–58% relative humidity environment with free access to water and food and a temperature of 22–25 °C on a 12 h light/dark cycle.

Rat Model of Sepsis and Experimental Groups

The rats (n = 187) were randomly divided into the following groups: Sham group (n = 29), CLP group (n = 78), Munc18-1 siRNA (Munc18-1 si) group (n = 40), and Munc18-1 siRNA control (Munc18-1 si-c) group (n = 40).

The dose of the administered drug in the same volume was verified during the pre-experimental phase. At 2 d before CLP, the Munc18-1 si group were injected with 5 ul Munc18-1 siRNA transfection complex in the lateral ventricle, and the Munc18-1 si-c group were injected with 5 ul control siRNA transfection complex. The Munc18-1 siRNA and control siRNA were synthesized by Ruibo Biotech (Guangzhou, China). The sequence chain of Munc18-1 siRNA was 5'-GCATCATCCTTCTCTACAT-3'. To prepare the transfection complex, the EntransterTM-in vivo(Engreen Biosystem, China) reagent was diluted with normal saline and added to a nucleic acid solution diluted to 1 ug/ul with non-toxic pure water (volume ratio of nucleic acid: transfection reagent = 2:1). After anesthetizing the rat with 100% O2 isoflurane (induction dose 2%, maintenance dose 1%), the rat's head was fixed with a prone position on a stereotaxic device. Based on the left and right cochlear connection, the central axis of the head was defined as the direction, and the hair on the middle of the rat's head was cut and sterilized, such that 1 cm of the skin and the subcutaneous fascia were cut with the blade to expose the skull. At 8 mm from the bregma and 2 mm from the right side of the midline, a dental drill was used to open the skull and pick up the dura mater. Then, a micro-pump syringe was used to insert the needle to a depth of 6 mm, and a bolus was injected at a speed of 1 ul/min. After finishing the injection, the needle was paused for 2 min and then slowly withdrew.

By performing the CLP, sepsis was established in the CLP, CLP + Munc18-1 si and CLP + Munc18-1 si-c

groups. After the rats were deeply anesthetized by inhalation isoflurane (induction dose 2%, maintenance dose 1%) in 100% O2, the abdominal area was shaved and disinfected, and then an incision was made along the midline of the abdomen. The cecum was dissociated, ligated and then punctured twice with 18-gauge needle. A small amount of feces was extruded before replacing it into the abdominal cavity. Then, the cecum was returned and the abdominal cavity was sutured layer by layer. In order to compensate for the blood volume lost during surgery, the rats were treated with 0.9% (w/v) saline (50 mL/kg). The rats of the Sham group underwent the same procedure without ligation, puncture or any other treatment.

Vital Signs Monitoring

The rats (each group n = 6) were continuously anesthetized by inhalation isoflurane (induction dose 2%, maintenance dose 1%) in 100% O_2. An indwelling catheter was placed in the femoral artery and connected to a biological signal recorder (iWorx Systems, Inc.), which was used to monitor the mean arterial pressure (MAP) and heart rate (HR).

Neurophysiological Assessment

The neurophysiological scoring (n = 6) was performed to observe their neural reflexes to confirm the development of SAE. The reflexes include the auricular reflex, corneal reflex, righting reflex, tail flick reflex and escape reflex over a specified time period. The scores were assigned as follows: in each reflex, 1 point for weakened reflexes (no reflexes within 10 s), 0 point for no reflexes, and 2 points for normal reflexes, according to a previous study [23].

Hematoxylin and Eosin (H&E) and Immunofluorescence Staining

After deep anesthesia, the rats (n = 6) were injected with 100 mL 0.9% (w/v) saline and 100 mL 4% (w/v) paraformaldehyde (PFA) into the left ventricle for cardiac perfusion. The brain tissue was fixed in 4% PFA, dehydrated with alcohol, cleared with xylene and embedded with paraffin. The sample was cut into 6-μm sections and dried. Afterwards, xylene was dewaxed and the sections were rehydrated through an alcohol series. Afterwards, two types of staining were performed. First, staining with H&E was performed, and the images were taken using the Leica inverted optical microscope (Leica, Mannheim, Germany).

Next, staining with immunofluorescence (n = 6) was performed. The slices were treated with 0.3% Triton 100 PBS solution for 30 min and fluorescent blocking solution for 1 h. The required primary antibodies, including the anti-Munc18-1 rabbit polyclonal antibody (1:50, ab3451, Abcam), anti-Syntaxin1A rabbit polyclonal antibody (1:25, ab41453, Abcam), anti-Synaptophysin mouse monoclonal antibody (1:50, ab8049, Abcam), anti-NMDAR1 rabbit polyclonal antibody (1:50, ab52177, Abcam), anti-NeuN mouse antibody (1:300, Abcam) and anti-NeuN rabbit antibody (1:300, Abcam) were incubated overnight in a refrigerator at 4 °C. After rinsing for 3 times in PBS solution on the next day, secondary antibodies were added, including the CY3 conjugated anti-rabbit IgG (1:500, Jackson ImmunoResearch, West Grove, PA, USA), CY3 conjugated anti-mouse IgG (1:500,Jackson ImmunoResearch, West Grove, PA, USA), Dy Light 488 conjugated anti-rabbit IgG (1: 500,Jackson ImmunoResearch, West Grove, PA, USA) and Dy Light 488 anti-mouse IgG (1:500,Jackson ImmunoResearch, West Grove, PA, USA), and then 4′,6-diamidino-2-phenylindole (DAPI) (1:500, Beyotime) was added followed by incubation for 1 h in the dark. The sections were sealed on a glass slide with an anti-fluorescence quencher (Beyotime). Finally, the images were taken using the Pannoramic MIDI digital section scanner (3DHistechxyl, Hungary).

Transmission Electron Microscopy

After deep anesthesia, the rats (n = 5) were injected with 100 mL 0.9% (w/v) saline and 100 mL 2% glutaraldehyde into the left ventricle for cardiac perfusion. Hippocampus tissues were placed with the size of rice grains in 2.5% glutaraldehyde solution, washed with PBS, fixed in a phosphate buffered osmium tetroxide solution containing 30 g/L glutaraldehyde and embedded in epoxy resin. The brain tissue was cut into 0.12 μm slices and stained with 2 g/L lead citrate and 10 g/L uranyl acetate. The synaptic structure of the hippocampal neurons and number of synaptic vesicles in the synaptic active area were observed using a transmission electron microscopy. On the inside of the presynaptic membrane, there is a fence-like structure, also called the synaptic active area, where the synaptic vesicles discharge neurotransmitters, and some receptor proteins gather under the postsynaptic membrane to form postsynaptic density (PSD) [24]. The typical excitatory synapse structure is shown as follows [24]: (1) The thickness of the postsynaptic membrane is much larger than that of the presynaptic membrane; (2) The PSD can be seen in the postsynaptic membrane; (3) Round and clear synapse vesicles are observed in the presynaptic membrane. A total of 15 typical excitatory synaptic structures were selected from each specimen. The Image J software (NIH, Bethesda, MD, USA) was used to quantify the distance of 150 nm from the presynaptic membrane of the synaptic active area, and then the number of vesicles in the synaptic active area was observed by HT7700 120 kV TEM (Hitachi, Tokyo, Japan).

Western Blotting (WB)

After deep anesthesia at a specific time point, the brains (n = 6) of the rats were quickly removed. The hippocampal tissue separated on ice was added to the freshly prepared solution consisting of Radio Immunoprecipitation Assay Lysis Buffer, Phenylmethanesulfonyl fluoride and Aprotinin for 30 min and was then broken by a tissue crusher. After placing the samples on ice for 30 min, they were centrifuged in a high-speed refrigerated centrifuge (4 °C, 14,000 rpm) for 30 min. Next, the supernatant was extracted, the loading buffer (Beyotime, Shanghai, China) was added in proportion, and the denaturation was performed at a high temperature of 100 °C for 10 min. To ensure the consistency of the protein content in each sample, the BCA analysis kit (Beyotime) was used to determine the protein content in the denatured sample. Afterwards, the deformed and cooled sample (Add 5ug to each well) was electrophoresed on a prepared SDS-polyacrylamide gel and transferred to a methanol-excited polyvinylidene fluoride (PVDF) membrane (Millipore, Billerica, MA, USA). After taking out the PVDF, it was immersed in 5% milk sealing liquid and sealed for 1 h. Then, the PVDF was incubated with primary antibodies, including the anti-Munc18-1 rabbit polyclonal antibody (1:1000, ab3451, Abcam), anti-Syntaxin1A rabbit polyclonal antibody (1:1000, ab41453, Abcam), anti-Synaptophysin mouse monoclonal antibody (1:500, ab8049, Abcam), anti-NMDAR1rabbit polyclonal antibody (1:1000, ab52177, Abcam), anti-β-actin mouse monoclonal antibody (1:5000, ZSGB-BIO, Beijing, China), anti-GAPDH mouse monoclonal antibody (1:5000, ZSGB-BIO, Beijing, China) and anti-β-tubulin mouse monoclonal antibody (1:5000, ZSGB-BIO, Beijing, China) in a refrigerator overnight at 4 °C. On the next day, the PVDF was rinsed with TBST for 3 times, then it reacted with the corresponding secondary antibodies, including the HRP-labeled anti-rabbit or anti-mouse IgG, and was incubated for 1 h and then rinsed with TBST for 3 times. The bands were visualized using enhanced chemiluminescence (Millipore) and imaged using a gel imaging analysis system (Bio-Rad, Hercules, CA, USA). The intensity of each band was quantitatively analyzed by the Image Lab software. The resulting density ratio represents the relative expression of each band against GAPDH, β-actin and β-tubulin.

Liquid Chromatograph Mass Spectrometer (LC/MS) Method

A sufficient amount of glutamate standard substance was accurately weighed, and a 1 mg/ml stock solution with methanol was prepared. The prepared stock solution was diluted into a standard curve working solution with a series of concentration gradients. The obtained concentration was separately 50 ug/ml, 20 ug/ml, 5 ug/ml, 0.5 ug/ml. Then, 500 ul solution (the hippocampal tissue solutions were prepared with using methanol plus 0.1% formate) was added to the hippocampus specimen (n = 6) and vortexed to mix for 5 min, centrifuged in a centrifuge (12,000 rpm, 10 min). The supernatant was diluted to 20 times and analyzed. The Xcalibur 3.0 software was used to process the chromatogram collection of glutamate (Column: Thermo Hypersil GOLD HILIC 100 × 2.1 mm, 1.9 μm; Flow rate: 0.45mL/min; Time: 5 min). The standard curve was obtained by regression with weighting coefficient ($1/X^2$) with taking the peak area of glutamate as the ordinate and the concentration of glutamate as the abscissa.

Statistical Analysis

The values used in the experimental results were expressed as mean ± standard error of mean (SEM) for at least 5 rats. The SPSS version 23.0 software (SPSS, Inc., Chicago, IL, USA) was used for statistical analysis. The statistical significance of differences between groups was analyzed by one-way analysis of variance followed by the Student-Newman-Keuls post-hoc test. $P < 0.05$ was considered to be statistically significant.

Results

Establishment of a Septic Rat Model

To verify whether CLP successfully induced sepsis in rats, some assessments were conducted. The CLP group had a postoperative mortality rate of 9.3% at 12 h, 25.58% at 24 h and 32.55% at 48 h. The MAP (mmHg) gradually decreased, with the lowest point at 24 h (Sham vs. CLP: 99.83 ± 4.45 vs. 68.67 ± 9.75, $P < 0.01$), while the heart rate (beats/min) gradually increased, with peak point at 24 h (Sham vs. CLP: 379.33 ± 11.76 vs. 471 ± 20.54, $P < 0.01$) (Fig. 1a). At the same time, the CLP group showed less movement, erected hair, shaking and curling up. Moreover, neurophysiological scores of the CLP group decreased (Sham vs. CLP: 10 ± 0 vs. 5.17 ± 0.75, $P < 0.01$) (Fig. 1a). The pathological changes of the hippocampus in the CLP group showed disordered cell arrangement and abnormal morphology (Fig. 1b). These findings are in accordance with the findings by Kafa et al. [25], suggesting that the model of sepsis was successfully established.

Abnormal Glutamate Levels in the Hippocampus of Septic Rats

We observed the changes of glutamate in hippocampal neurons of septic rats. First, using LC-MS, we found that

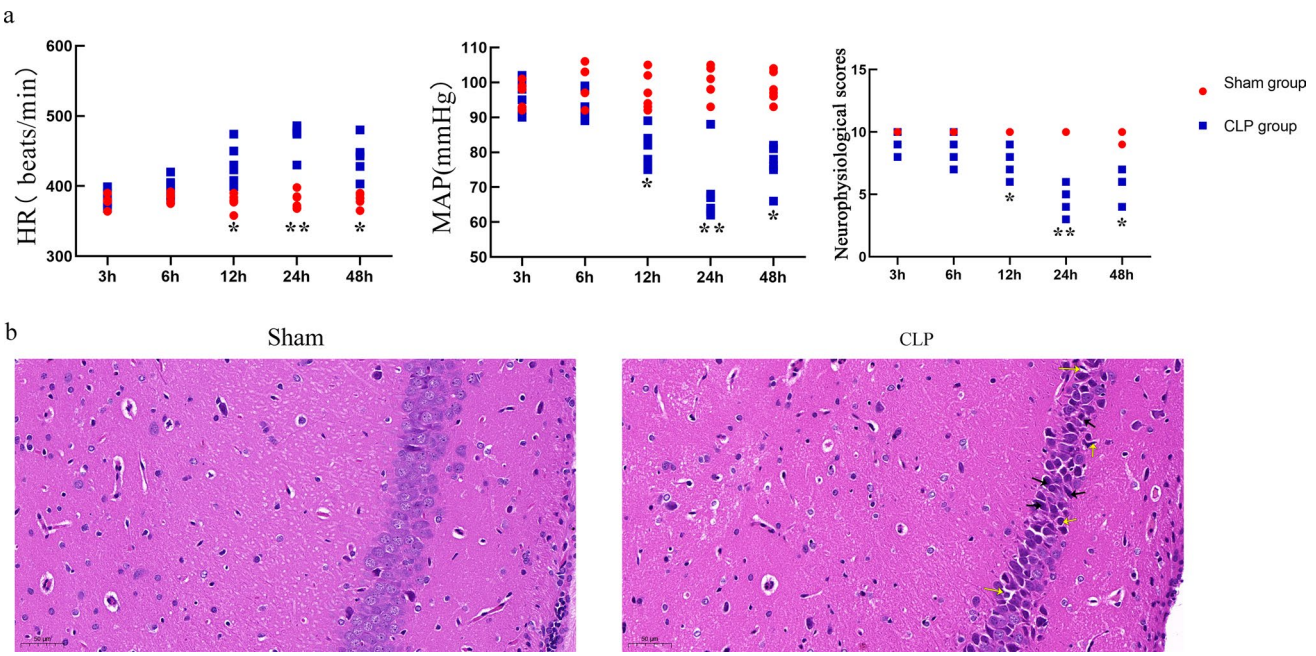

Fig. 1 The vital signs, neurophysiological scores and histopathological changes in the hippocampus in each group
a the HR of CLP gradually increased, the MAP and neurophysiological scores gradually decreased, which was obvious at 24 h, compared with Sham; **b** Pathological changes of the hippocampus detected in each group at 24 h. Sham group were normal and orderly, with normal morphology, and a large number of clearly visible nucleoli. CLP group were degenerated and swollen, with irregular cell boundaries, disordered cell arrangement, deep staining of the cytoplasm (black arrow), and Pyknosis of the nucleus to form a vacuole structure (yellow arrow). scale bar = 50 μm. (n = 6 for each group. $P^* < 0.05$ VS Sham, $P^{**} < 0.01$ VS Sham)

the content of glutamate (ug/mg) in the hippocampus of the CLP group increased (Sham vs. CLP: 3.792 ± 0.513 vs. 4.638 ± 0.562, P < 0.05) (Table 1). Excitatory neuronal synapses were then visualized using transmission electron microscopy, quantified as the 150 nm distance to the active area of the presynaptic membrane, where an increased number of synaptic vesicles was found (Sham vs. CLP: 10.53 ± 0.47 vs. 18.76 ± 2.31, P < 0.05) (Fig. 2a). Finally, we monitored the expression of the postsynaptic membrane glutamate receptor NMDAR1 using WB and immunofluorescence and found that the expression increased (Sham vs. CLP: 0.46 ± 0.05 vs. 1.13 ± 0.21, 1.09 ± 0.2 vs. 1.63 ± 0.30, P < 0.05) (Fig. 2b, c). These findings suggest that glutamate level in the hippocampus of rats is increased during sepsis.

Increased Expression of Munc18-1, Syntaxin1A and Synaptophysin in the Hippocampus of Septic Rats

Munc18-1, Syntaxin1A and Synaptophysin regulate neurotransmitter transmission. The WB results showed that the expressions of Munc18-1, Syntaxin1A and Synaptophysin increased in the CLP group (Sham vs. CLP: 0.61 ± 0.79 vs. 1.53 ± 0.13, 2.17 ± 0.23 vs. 3.23 ± 0.33, 0.61 ± 0.08 vs. 0.90 ± 0.18, P < 0.05) (Fig. 3a, b, c). In addition, the immunofluorescence results at 24 h after surgery showed that the fluorescence signals of Munc18-1, Syntaxin1A, and Synaptophysin in the CLP group were enhanced (Sham vs. CLP: 39.67 ± 9.63 vs. 58.34 ± 5.13, 43.52 ± 6.19 vs. 62.46 ± 14.32, 25.6 ± 3 2.21 vs. 44.34 ± 7.88, P < 0.05) (Fig. 3a, b, c), which was consistent with the WB results. These findings suggested that sepsis-induced upregulation of Munc18-1, Syntaxin1A and Synaptophysin in the hippocampus of rats.

Munc18-1 Regulates the Expression of Syntaxin1A and Synaptophysin in the Hippocampus of Septic Rats

At the presynaptic membrane, Munc18-1 interacts with Syntaxin1A and Synaptophysin to regulate the synaptic vesicle anchoring and fusion. To explore the relationship between Munc18-1, Syntaxin1A and Synaptophysin in hippocampus of septic rats, we used Munc18-1 siRNA to intervene in septic rats. Interestingly, WB results showed that the expressions levels of Munc18-1, Syntaxin1A and Synaptophysin in the hippocampus of the CLP + Munc18-1 si group decreased (CLP vs. CLP + Munc18-1 si: 0.33 ± 0.14 vs. 0.23 ± 0.22, 0.38 ± 0.03 vs. 0.28 ± 0.03, 0.96 ± 0.12 vs. 0.57 ± 0.11, P < 0.05) (Fig. 4a, b). In addition, immunofluorescence results showed that the fluorescence signals of Munc18-1, Syntaxin1A and Synaptophysin in the hippocampus

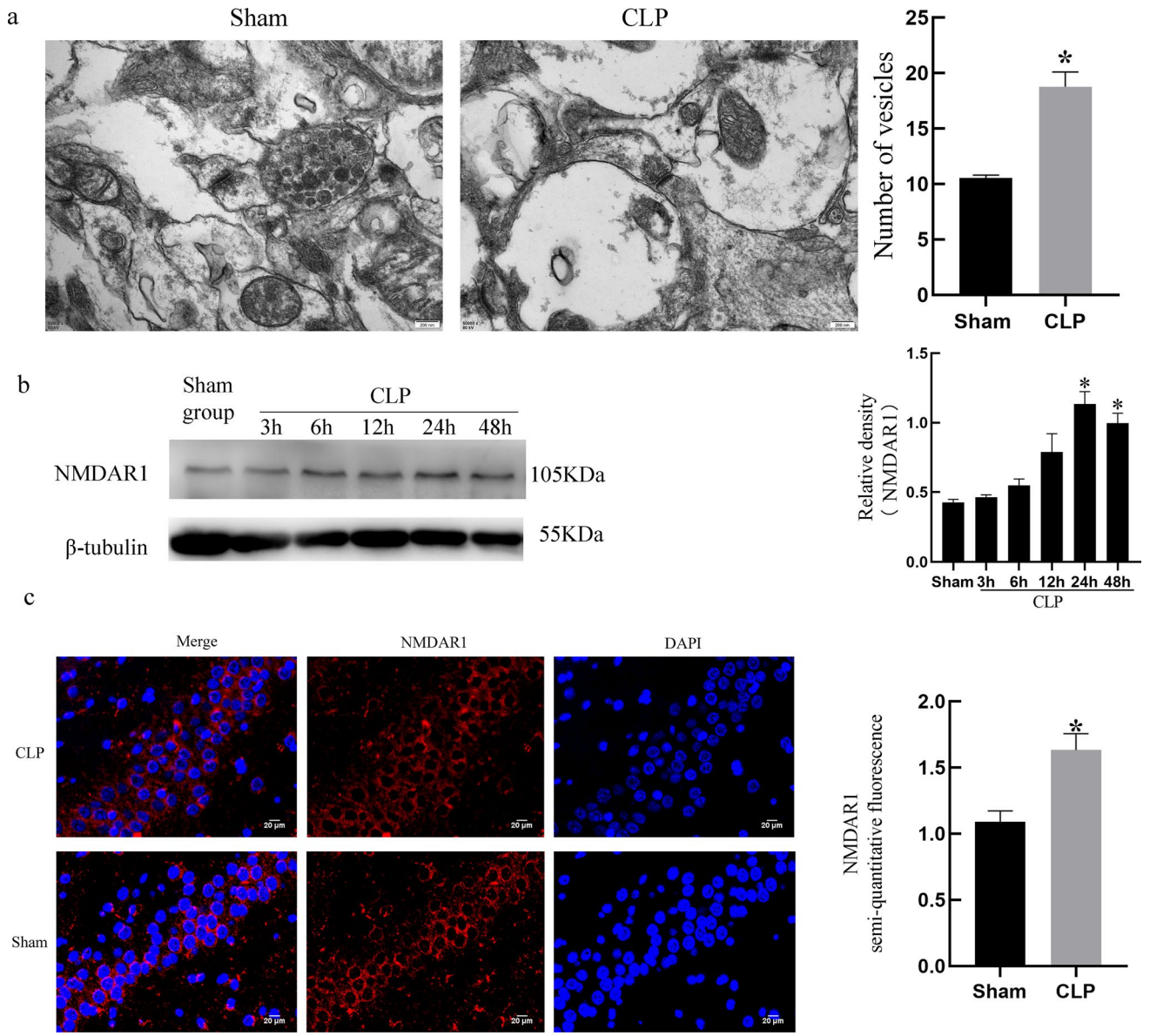

Fig. 2 Number of synaptic vesicles in the synaptic active area of hippocampal neurons and the expression of NMDAR1 after CLP.
a The synaptic structure of the hippocampal neurons and number of synaptic vesicles in the synaptic active area were observed with transmission electron microscope. The results showed synaptic structures in Sham and CLP, including the presynaptic membrane, synaptic cleft, postsynaptic membrane, postsynaptic dense area, round and transparent synaptic vesicles in the presynaptic membrane. The number of synaptic vesicles in the CLP increased at 24 h after surgery. The data are represented by histograms. Scale bar = 200 nm, n = 5. **b** The levels of NMDAR1 in hippocampus harvested at different time points after CLP were normalized to the levels of β-tubulin, and displayed as relatively arbitrary units; The expression of NMDAR1 increased. The protein content is represented by histograms. c, the fluorescence of NMDAR1 in the hippocampus at 24 h after CLP; The fluorescence signal of NMDAR1 in the CLP was enhanced. The coincidence rate is represented by histograms. Scale bar = 20 μm, n = 6. (P* < 0.05 VS Sham)

of rats in the CLP + Munc18-1 si group attenuated (CLP vs. CLP + Munc18-1 si: 55.13 ± 5.69 vs. 43.75 ± 2.75, 55.99 ± 0.85 vs. 44.03 ± 0.55, 41.54 ± 9.56 vs. 22.91 ± 3.76, P < 0.05) (Fig. 4a, b), which was consistent with the results of WB. These results show that the expressions levels of Syntaxin1A and Synaptophysin in the hippocampus of septic rats are regulated by Munc18-1.

Munc18-1 Regulates Glutamate Levels in Septic Rats

To investigate whether glutamate level in the hippocampus of septic rats is regulated by Munc18-1, we conducted a series of observations after Munc18-1 siRNA intervention in CLP. Firstly, the LC-MS monitoring showed that the content of glutamate (ug/mg) in the hippocampus of

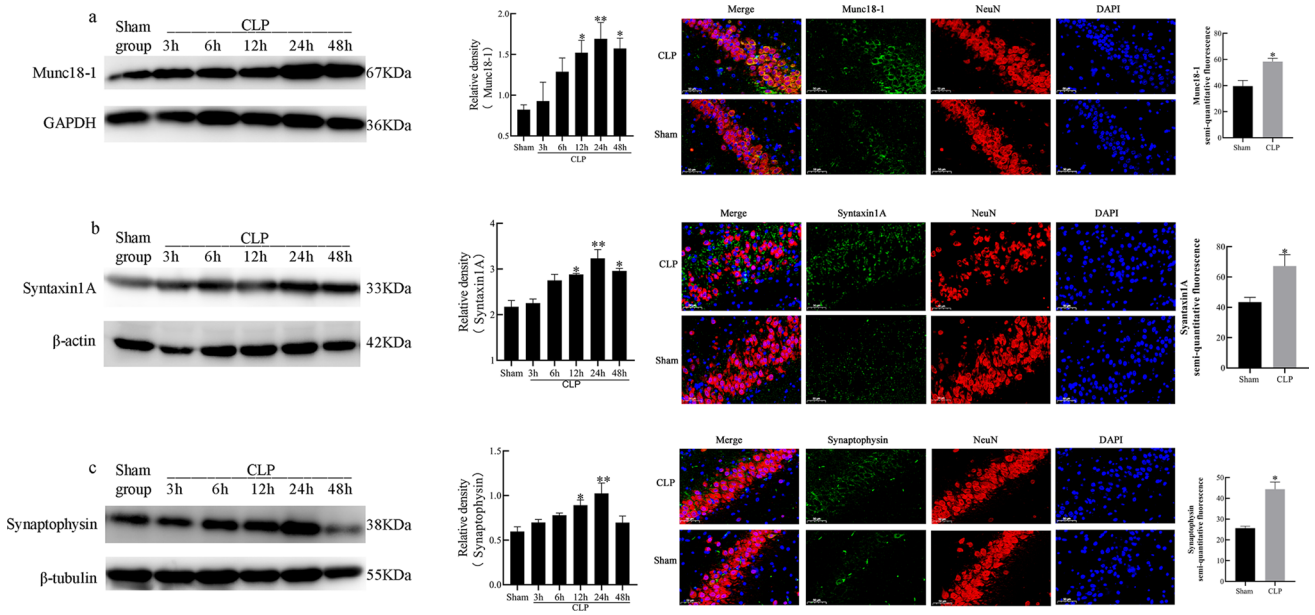

Fig. 3 The expression of Munc18-1, Synataxin1A and Synaptophysin at different time points after CLP.
a The level of Munc18-1 in hippocampus harvested at different time points after CLP was normalized to the level of GAPDH and displayed as relatively arbitrary units; The expression of the Munc18-1 increased; The fluorescence signal of Munc18-1 at 24 h after CLP was enhanced. **b** The level of Syntaxin1A harvested at different time points after CLP were normalized to the level of β-actin and displayed as relatively arbitrary units; The expression of the Syntaxin1A increased; The fluorescence signal of Syntaxin1A at 24 h after CLP was enhanced. c, the level of Synaptophysin harvested at different time points after CLP were normalized to the levels of β-tubulin and displayed as relatively arbitrary units; The expression of the Synaptophysin increased; The fluorescence signal of Synaptophysin at 24 h after CLP was enhanced. The protein content is represented by histograms. The coincidence rate of fluorescence signals is represented by histograms. Scale bar = 50 μm. (n = 6 in each group; P* < 0.05 VS Sham group, P** < 0.01 VS Sham group)

the CLP + Munc18-1 si group was decreased (CLP vs. CLP + Munc18-1 si: 4.638 ± 0.562 vs. 3.713 ± 0.442, P < 0.05) (Table 1). Secondly, the excitatory synapses of the hippocampal neurons were observed using transmission electron microscope, and the results showed that the number of synaptic vesicles in the synaptic active area of the CLP + Munc18-1 si group decreased (CLP vs. CLP + Munc18-1 si:17.56 ± 1.50 vs. 11.11 ± 1.50, P < 0.05) (Fig. 5a). Finally, we monitored the expression of the NMDAR1, and WB showed that the expression of NMDAR1 decreased in the CLP + Munc18-1 si group (CLP vs. CLP + Munc18-1 si: 0.78 ± 0.08 vs. 0.52 ± 0.09, P < 0.05) (Fig. 5b). Immunofluorescence showed that the fluorescence signal of CLP + Munc18-1 si group was attenuated (CLP vs. CLP + Munc18-1 si: 1.71 ± 0.25 vs. 1.19 ± 0.25, P < 0.05) (Fig. 5c). These results suggest that glutamate levels in hippocampal neurons of septic rats is regulated by Munc18-1.

Inhibition of Munc18-1 Expression Can Improve Vital Signs and Hippocampal Pathological Damage in Septic Rats

To evaluate the effect of Munc18-1 expression levels on the vital signs and hippocampal pathological changes during sepsis, several evaluations were performed after Munc18-1 siRNA interference in septic rats. The vital signs monitoring results showed that MAP (mmHg) increased, HR (beats/min) decreased, and neurophysiological scores increased in CLP + Munc18-1 si group (CLP vs. CLP + Munc18-1 si: 65.83 ± 5.30 vs. 91.83 ± 3.54, 478.33 ± 13.46 vs. 401 ± 14.66, 4.33 ± 0.82 vs. 8 ± 0.89, P < 0.05) (Fig. 6a, b, c). H&E results indicated that the pathological damage of hippocampus in CLP + Munc18-1 si group improved (Fig. 6d). The above-mentioned results indicate that targeted inhibition of Munc18-1 expression ameliorate the vital signs and the hippocampal injury of septic rats.

Discussion

Although sepsis has some commonalities in children and adults, some differences in the pathophysiological process still exist [26]. The children's immune system is still developing, and the lack of anti-inflammatory ability makes inflammation less likely to be localized, so they are prone to infection [27]. Compared with adults, they have a lower rate of multiple organ dysfunction, and hypotension develops later in children because the increased cardiac output in

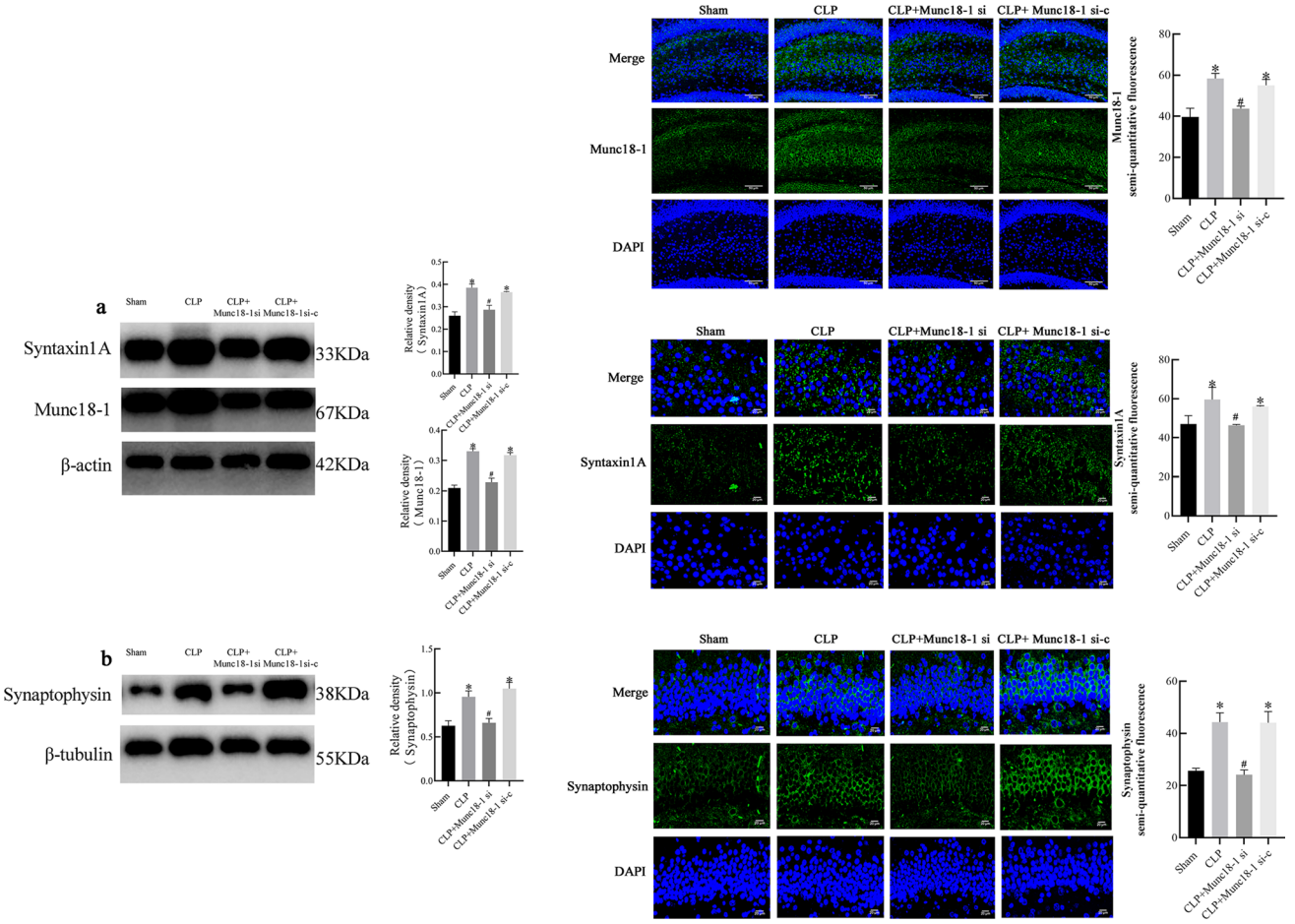

Fig. 4 Munc18-1siRNA down-regulated the protein levels of Syntaxin1A and Synaptophysin during sepsis

a The protein levels of Munc18-1 and Syntaxin1A in hippocampus harvested at 24 h after CLP were normalized to the level of β-actin and displayed as relatively arbitrary units; The expression of Munc18-1 and Syntaxin1A in the CLP and CLP + Munc18-1 si-c increased, compared with Sham; and decreased in the CLP + Munc18-1 si, compared with CLP. The fluorescence signals of Munc18-1 and Syntaxin1A in the CLP and CLP + Munc18-1 si-c were enhanced, compared with Sham; and were weakened in the CLP + Munc18-1 si, compared with CLP. **b** The protein level of Synaptophysin harvested at 24 h after CLP were normalized to the level of β-tubulinn and displayed as relatively arbitrary units; The expression of Synaptophysin in the CLP and CLP + Munc18-1 si-c increased, compared with Sham; and decreased in the CLP + Munc18-1 si, compared with CLP. The fluorescence signal of Synaptophysin in the CLP and CLP + Munc18-1 si-c group were enhanced, compared with Sham; and were weakened in the CLP + Munc18-1 si, compared with CLP. The protein content is represented by histograms; The coincidence rate of fluorescence signals is represented by histograms. Scale bar = 20 or 50 μm. Values are expressed as mean ± SEM. (n = 6 in each group; $P^{*} < 0.05$ VS Sham, $P^{\#} < 0.05$ VS CLP).

children through a very rapid heart rate can be maintained for a long time without myocardial ischemia [27]. In this study, 30-day rats were selected to simulate the development of childhood with sepsis through CLP. Compared with the Sham group, the rats in the CLP group, with erecting hairs and shaking, had decreased MAP, increased HR and a certain mortality rate. The above-mentioned results indicate the successful establishment of the sepsis rat model through CLP. H&E staining showed that the hippocampus of the rats in the CLP group had aggravated pathological changes and decreased neurophysiological scores. The results suggest that hippocampal damage in rats can be induced by the establishment of a sepsis model by CLP. A previous study showed that the hippocampus of rats was injured during sepsis, and it was obvious at 12–24 h after surgery [28]. Interestingly, our results showed similar findings.

Altered neurotransmitter levels in the brain are a key factor in SAE, and inflammatory processes promote changes in many neurotransmitter systems, including glutamatergic, monoaminergic, and cholinergic [29]. Glutamate represents the main excitatory neurotransmitter in the central nervous system, and excessive levels of synaptic glutamate can over-activate NMDAR to produce excitotoxicity and damage the nerual cells [30]. NMDAR is an ionotropic glutamate

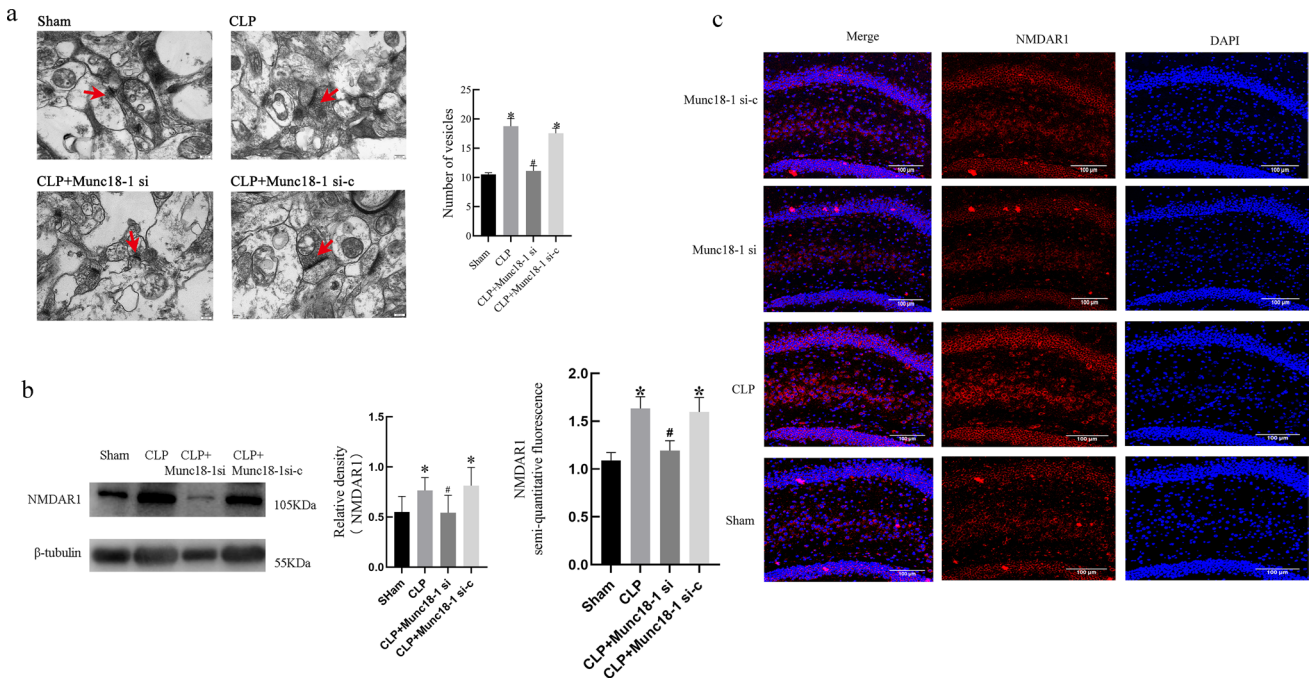

Fig. 5 Munc18-1siRNA inhibited glutamate levels
a Number of synaptic vesicles in each group. The results showed round and transparent synaptic vesicles (red arrows) in the presynaptic membrane in each group. The number of synaptic vesicles of Munc18-1, Syntaxin1A and Synaptophysin in the CLP and CLP + Munc18-1 si-c increased, compared with Sham; and decreased in the CLP + Munc18-1 si, compared with CLP. The data are represented by histograms. Scale bar = 200 nm, n = 5. **b** The protein level of NMDAR1 harvested at 24 h after CLP were normalized to the level of β-tubulinn and displayed as relatively arbitrary units; The expression of NMDAR1 in the CLP and CLP + Munc18-1 si-c increased, compared with Sham; and decreased in the CLP + Munc18-1 si, compared with CLP. **c** The fluorescence signal of NMDAR1 in the CLP and CLP + Munc18-1 si-c were enhanced, compared with Sham ; and were weakened in the CLP + Munc18-1 si, compared with CLP. The protein content is represented by histograms; The coincidence rate of fluorescence signals is represented by histograms. Scale bar = 20 or 50 μm, n = 6. Values are expressed as mean ± SEM. ($P^* < 0.05$ VS Sham, $P^{\#} < 0.05$ VS CLP).

receptor with an important role in the regulation of neuronal survival and synaptic plasticity, of which NMDAR1 is the main subtype constituting ion channels [31]. Excessive activation of NMDARs leads to Ca^{2+} overload and Na^{+} accumulation in neural cells, which induces the activation of various signaling pathways and enzymes including proteases, kinases, phosphokinases, lipoxygenases, NOS and ROS, leading to neuronal necrosis and apoptosis [31]. It has been found that transient forebrain ischemia under hyperthermic conditions accelerates memory impairment and neuronal death in the mouse hippocampus due to increased NMDAR1 expression, which is associated with increased hippocampal glutamate levels [32]. A previous study on sepsis-related hearing impairment found that the basal portion of the cochlear intimal cells in septic mice exhibited glutamate excitotoxicity [33]. In addition, another study showed that glutamate levels in brain tissue fluid increased during SAE and exerted excitotoxic effects on nerve cells by activating NMDARs [34]. In this study, we observed increased glutamate content and NMDAR1 expression in the hippocampus of septic rats. This suggests that the glutamate/NMDAR1 pathway is activated during sepsis. NMDARs are mainly located in the postsynaptic membrane [11]. Our results appear to suggest abnormal glutamate transmission during sepsis. However, It has been reported that NMDAR is also expressed in the presynaptic membrane [11]. Therefore, the determination of NMDAR1 expression at the postsynaptic membrane is required to further elucidate the role of abnormal glutamate transmission in SAE. In addition, although the specific mechanism of excitotoxicity is unclear, it was found that glutamate transporter-1 (GLT-1), the main glutamate transporter in brain tissue, affects glutamate excitotoxicity [35]. GLT-1 is a major transporter in the brain, which is expressed in both glial cells and neurons, but to a lesser extent in neurons [36]. A previous study has shown that the deletion of the GLT-1 gene abolishes 95% of the glutamate uptake activity in forebrain synaptosome [37]. During sepsis, brain tissue glutamate release is increased and uptake is decreased [9, 10]. Therefore, the determination of GLT-1 can further illustrate the role of glutamate excitotoxicity in hippocampal injury in septic rats. Unfortunately, due to limited technology equipment and the Covid-19 pandemic.

The anchoring and fusion of synaptic vesicles is the basic process of neurotransmitter transmission, and the increase

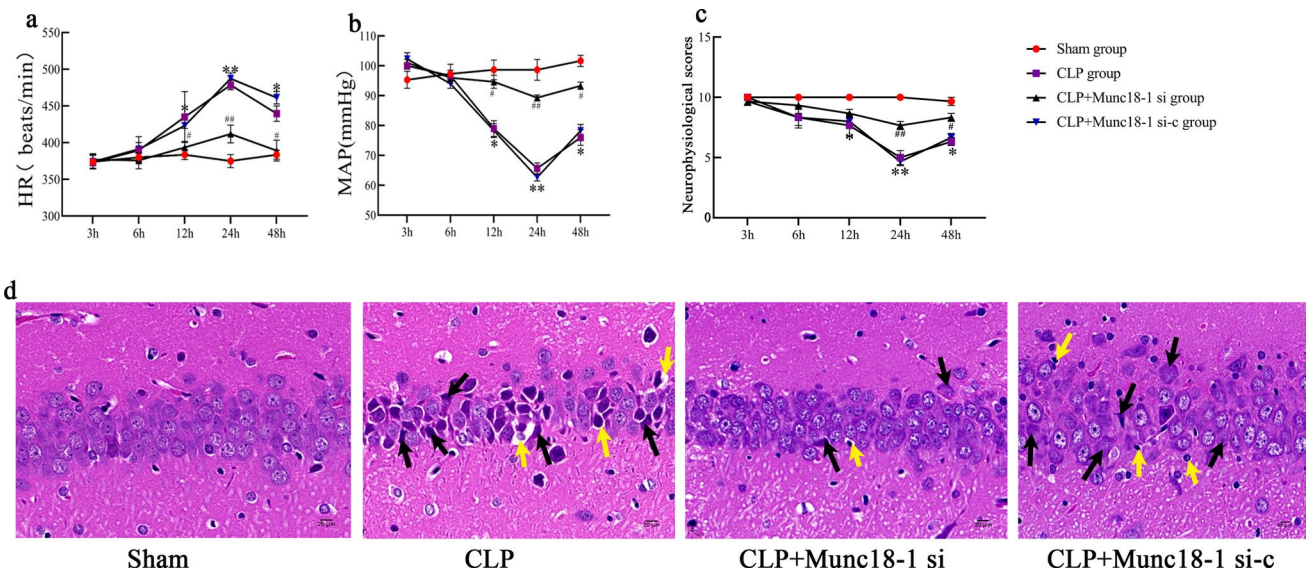

Fig. 6 Inhibition of Munc18-1 expression improve vital signs and hippocampal pathological damage in septic rats

a HR; **b** MAP; **c** neurophysiological scores; the HR of CLP and CLP + Munc18-1 si-c gradually increased, the MAP and neurophysiological scores gradually decreased, which was obvious at 24 h, compared with Sham; the HR of CLP + Munc18-1 si group decreased, the MAP and neurophysiological scores increased, compared with CLP. **d** Pathological changes of the hippocampus detected in each group at 24 h. Sham group were normal and orderly, with normal morphology, and a large number of clearly visible nucleoli. CLP and CLP + Munc18-1 si-c group were degenerated and swollen, with irregular cell boundaries, disordered cell arrangement, deep staining of the cytoplasm (black arrow), and pyknosis of the nucleus to form a vacuole structure (yellow arrow); the CLP + Munc18-1 si group were normal and orderly, with a slightly normal morphology, with more clearly visible nucleoli, and occasionally deep staining of the cytoplasm (black arrow) and vacuole structure (yellow arrow). scale bar = 20 μm (n = 6 for each group. $P^{*} < 0.05$ VS Sham, $P^{**} < 0.01$ VS Sham, $P^{\#} < 0.01$ VS CLP, $P^{\#\#} < 0.01$ VS CLP).

in the number of synaptic vesicles in the synaptic active area is positively correlated with the amount of released neurotransmitters [38]. A previous study on a mouse model of heterozygous knockout of the *STXBP1* gene found that the number of synaptic vesicles in the synaptic active area decreased with decreased expression of Munc18-1, and the transmission of glutamatergic and GABAergic signals was impaired [39]. As the expression of Munc18-1 increased, the number of synaptic vesicles increased, and its expression level reflected the change in the number of synaptic vesicles in the synaptic active area [16]. The activation of the diacylglycerol (DAG)/protein kinase C (PKC) pathway can promote the conversion of the Syntaxin1-Munc18-1 dimer to the assembled SNARE complex, enhancing the neurosynaptic transmission process [40]. In addition, this pathway also promotes the phosphorylation of Munc18-1 to transfer the synaptic vesicles to the active area [41]. Another study concluded that riluzole attenuated the neurological symptoms in septic rats by inhibiting glutamate release into the synaptic cleft [42]. Riluzole mainly inhibited the PKC pathway/phosphorylation of the Munc18-1 to reduce the level of vesicles in the synaptic active area and inhibit the presynaptic release of glutamate to play a protective role [43]. In this work, we observed an increase in the number of synaptic vesicles in areas of synaptic activity in neurons with excitatory synaptic structures. Interestingly, the down-regulation of Munc18-1 expression with Munc18-1 siRNA decreased the number of synaptic vesicles in the synaptic active area, as well as the glutamate content and NMDAR1 expression in the hippocampus of septic rats. Therefore, our findings suggest that Munc18-1 may be involved in neuronal damage by regulating the level of glutamate to induce excitotoxicity in the hippocampus of septic rats.

Munc18-1 mainly regulates the SNARE function by combining Syntaxin1 to affect the anchoring and fusion of the synaptic vesicles and the neurotransmitter transmission [44]. A previous study on patients with schizophrenia revealed that the expression of Syntaxin1A and Munc18-1 protein increased in their prefrontal cortex. Specifically, the expression of Syntaxin1A was upregulated by Munc18-1 [45]. A study on the heart regulation mechanism on sepsis reported that at 24 h after CLP, the expression of Syntaxin1A in the rat myocardial tissue increased, then decreased at 72 h [46]. In the experiment, WB and immunofluorescence detected an increased expression of Syntaxin1A of CLP group, which decreased after the intervention with Munc18-1 siRNA. The results showed that the expression of Syntaxin1A could be induced by CLP and regulated by Munc18-1. Synaptophysin plays an important role in regulating the neurotransmitter release, and its expression level reflects the number

of synaptic vesicles released through exocytosis [47, 48]. In this work, the results of WB and immunofluorescence revealed an increase in the expression of Synaptophysin of CLP group, which decreased after the intervention with Munc18-1 siRNA. The above-mentioned results indicated that CLP induced an increase in the expression of Synaptophysin in the hippocampus of rats. Munc18-1 could regulate the expression of Synaptophysin of septic rats to affect the activity of the synaptic vesicles. However, in a previous study, WB of the hippocampus and frontal cortex of septic rats that survived at 30 d after CLP, showed increased β-amyloid protein expression and decreased Synaptophysin expression [49]. Besides, in a study on simvastatin and rats that survived sepsis with long-term cognitive deficits suggested that the expression of Synaptophysin in the hippocampus of the CLP group decreased at 10 d after CLP [50]. This seems inconsistent with our results, but we speculate that it may be related to the short observation time point of this experiment. Our results suggested that Synaptophysin level increased at 24 h after surgery and then started to decrease at 48 h after surgery. Whether Synaptophysin will continue to decrease after 48 h needs to be further explored.

Our data showed that the rats had aggravated pathological damage in the hippocampus, increased HR, decreased MAP and neurophysiological scores during sepsis. After intervening with Munc18-1 siRNA, improvements were seen in the pathological damage in the hippocampus, neurophysiological scores and deteriorating vital signs. The above-mentioned results indicated that the expression level of Munc18-1 played an important role in the brain injury of septic rats. In the acute phase of sepsis, the pathological damage of SAE may be improved by reducing the expression of Munc18-1. Based on a previous study, the view suggested that the increased expression of Munc18-1 could induce the excitotoxicity of glutamate to damage nerve cells, while the decreased expression could damage the synaptic plasticity to affect the balance of glutamate, GABA, dopamine, and other neurotransmitters to impair learning and memory [39]. In our study, in the acute sepsis phase, the expression of Munc18-1 increased to a peak at 24 h after surgery and began to decline after 48 h. However, the observation time of the experiment was short, and we did not explore the expression of Munc18-1 at the stage of sepsis after 48 h. Therefore, further research is needed to study whether the expression of Munc18-1 will show a continuous decline, and play a role in long-term cognitive and learning ability dysfunction of patients surviving SAE.

Prospects and Shortcomings

Taken together, our findings suggest that Munc18-1 is involved in the pathological process of SAE by affecting glutamate level via regulating the expression of Syntaxin1A and Synaptophysin. Targeted down-regulation of Munc18-1 ameliorated brain injury in septic rats, being a process that may be associated with suppressed glutamate excitotoxicity. This provides a new target for the clinical treatment of SAE. Although our findings are meaningful, they also reveal some deficiencies and limitations. The next step is to verify the direct relationship between Munc18-1 and the content of glutamate in the synaptic cleft through in vitro cell experiments, and to observe whether the overexpression of Munc18-1 in septic rats will aggravate hippocampal damage, further indicating that Munc18-1 is involved in target role in sepsis. In addition, the link between glutamate excitotoxicity and septic rat hippocampal neuronal cell death, such as apoptosis, needs to be further verified.

Table 1 The content of glutamate in hippocampus in each group.

Data are means ± SEM, n = 6 for each group. $P^{*} < 0.05$ VS Sham, $P^{\#} < 0.05$ VS CLP.

Group	Glutamate content in the hippocampus($\bar{x} \pm s$) ug/mg
Sham	3.792 ± 0.513
CLP	4.638 ± 0.562*
CLP + Munc18-1 si	3.713 ± 0.442$^{\#}$
CLP + Munc18-1 si-c	4.548 ± 0.59*

Author Contributions FJT conducted all the experiments and conducted the statistical analysis. FJT and LC drafted the manuscript, HG and LLP participated in the design of the study. LC, YPL and LLP participated in the physiological examination. DQX and XHL designed the project and finalized the manuscript. All authors read and approved the final manuscript. Thank EditSprings (https://www.editsprings.com) for editing English language of our manuscript.

Funding The present study was supported by the National Key R&D Program of China (Grant Nos. 2017YFA 0104201 and 2017YFA 0104200), the National Science Foundation of China (Grant Nos. 82071353, 82001593, 81330016, 81630038 and 81771634), and the Science and Technology Bureau of Chengdu City (Grant No. 2015-HM01-00424-SF).

Data Availability No additional data are available.

Conflict of interest

The authors declare that they have no competing financial interests or funding to disclose.

Declarations

Ethical Approval and Consent to Participate See methods section "Animals and treatments."

Consent for Publication Not applicable.

References

1. Napolitano LM (2018) Sepsis 2018: Definitions and Guideline Changes. Surg Infect (Larchmt) 19:117–125
2. Chung H-Y, Wickel J, Brunkhorst FM, Geis C (2020) Sepsis-associated encephalopathy: from delirium to dementia? J Clin Med 9:1
3. Sonneville R, Derese I, Marques MB, Langouche L, Derde S, Chatre L, Chrétien F, Annane D, Sharshar T, Van den Berghe G, Vanhorebeek I (2015) Neuropathological Correlates of Hyperglycemia During Prolonged Polymicrobial Sepsis in Mice. Shock 44:245–251
4. Zheng J, Luo F, Guo N-n, Cheng Z-y, Li B-m (2015) β1-and β2-adrenoceptors in hippocampal CA3 region are required for long-term memory consolidation in rats. Brain Res 1627:109–118
5. Pan C, Si Y, Meng Q, Jing L, Chen L, Zhang Y, Bao H (2019) Suppression of the RAC1/MLK3/p38 Signaling Pathway by β-Elemene Alleviates Sepsis-Associated Encephalopathy in Mice. Front Neurosci 13:358
6. Mazeraud A, Righy C, Bouchereau E, Benghanem S, Bozza FA, Sharshar T (2020) Septic-Associated Encephalopathy: a Comprehensive Review. Neurotherapeutics 17:392–403
7. Tauber SC, Djukic M, Gossner J, Eiffert H, Brück W, Nau R (2020) Sepsis-associated encephalopathy and septic encephalitis: an update. Expert Rev Anti Infect Ther 19:215–231
8. Czempik PF, Pluta MP, Krzych ŁJ (2020) Sepsis-Associated Brain Dysfunction: A Review of Current Literature.Int J Environ Res Public Health17
9. Kitagawa Y, Nakaso K, Horikoshi Y, Morimoto M, Omotani T, Otsuki A, Inagaki Y, Sato H, Matsura T (2019) System xc – in microglia is a novel therapeutic target for post-septic neurological and psychiatric illness. Sci Rep 9:7562
10. del Arroyo AG, Hadjihambi A, Sanchez J, Turovsky E, Kasymov V, Cain D, Nightingale TD, Lambden S, Grant SGN, Gourine AV, Ackland GL (2019) NMDA receptor modulation of glutamate release in activated neutrophils. EBioMedicine 47:457–469
11. Flores-Soto M, Chaparro-Huerta V, Escoto-Delgadillo M, Vazquez-Valls E, González-Castañeda R, Beas-Zarate C (2012) [Structure and function of NMDA-type glutamate receptor subunits]. Neurologia 27:301–310
12. Ramanathan M, Abdul KK, Justin A (2016) Low dose of l-glutamic acid attenuated the neurological dysfunctions and excitotoxicity in bilateral common carotid artery occluded mice. Behav Pharmacol 27:615–622
13. Salmasi M, Loebel A, Glasauer S, Stemmler M (2019) Short-term synaptic depression can increase the rate of information transfer at a release site. PLoS Comput Biol 15:e1006666
14. Blackwell KT, Ullrich A, Böhme MA, Schöneberg J, Depner H, Sigrist SJ, Noé F (2015) Dynamical Organization of Syntaxin-1A at the Presynaptic Active Zone. PLoS Comput Biol 11:e1004407
15. Romaniello R, Saettini F, Panzeri E, Arrigoni F, Bassi MT, Borgatti R (2015) A de-novo STXBP1 gene mutation in a patient showing the Rett syndrome phenotype. NeuroReport 26:254–257
16. Toonen RFG, Wierda K, Sons MS, de Wit H, Cornelisse LN, Brussaard A, Plomp JJ, Verhage M (2006) Munc18-1 expression levels control synapse recovery by regulating readily releasable pool size. Proceedings of the National Academy of Sciences 103:18332–18337
17. Gasman S, Gordon SL, Harper CB, Smillie KJ, Cousin MA (2016) A Fine Balance of Synaptophysin Levels Underlies Efficient Retrieval of Synaptobrevin II to Synaptic Vesicles. PLoS ONE 11:e0149457
18. Cousin MA, Evans GJO (2005) Tyrosine phosphorylation of synaptophysin in synaptic vesicle recycling. Biochem Soc Trans 33:1350–1353
19. Stamberger H, Weckhuysen S, De Jonghe P (2017) STXBP1 as a therapeutic target for epileptic encephalopathy. Expert Opin Ther Targets 21:1027–1036
20. Behan Á, Byrne C, Dunn MJ, Cagney G, Cotter DR (2008) Proteomic analysis of membrane microdomain-associated proteins in the dorsolateral prefrontal cortex in schizophrenia and bipolar disorder reveals alterations in LAMP, STXBP1 and BASP1 protein expression. Mol Psychiatry 14:601–613
21. Quinn R (2005) Comparing rat's to human's age: how old is my rat in people years? Nutrition (Burbank, Los Angeles County. Calif) 21:775–777
22. Ghasemi A, Jeddi S, Kashfi K (2021) The laboratory rat: Age and body weight matter. EXCLI J 20:1431–1445
23. Rittirsch D, Huber-Lang M, Flierl M, Ward PJNp (2009) Immunodesign of experimental sepsis by cecal ligation and puncture. 4:31–36
24. Rollenhagen A, Lübke JJC (2006) The morphology of excitatory central synapses: from structure to function. 326:221–237research t
25. Kafa I, Bakirci S, Uysal M, Kurt MJBr (2010) Alterations in the brain electrical activity in a rat model of sepsis-associated encephalopathy. 1354:217–226
26. Emr BM, Alcamo AM, Carcillo JA, Aneja RK, Mollen KP (2018) Pediatric Sepsis Update: How Are Children Different? Surg Infect (Larchmt) 19:176–183
27. Weiss S, Peters M, Alhazzani W, Agus M, Flori H, Inwald D, Nadel S, Schlapbach L, Tasker R, Argent A, Brierley J, Carcillo J, Carrol E, Carroll C, Cheifetz I, Choong K, Cies J, Cruz A, De Luca D, Deep A, Faust S, De Oliveira C, Hall M, Ishimine P, Javouhey E, Joosten K, Joshi P, Karam O, Kneyber M, Lemson J, MacLaren G, Mehta N, Møller M, Newth C, Nguyen T, Nishisaki A, Nunnally M, Parker M, Paul R, Randolph A, Ranjit S, Romer L, Scott H, Tume L, Verger J, Williams E, Wolf J, Wong H, Zimmerman J, Kissoon N, Tissieres P (2020) Surviving Sepsis Campaign International Guidelines for the Management of Septic Shock and Sepsis-Associated Organ Dysfunction in Children. Pediatric critical care medicine: a journal of the Society of Critical Care Medicine and the World Federation of Pediatric Intensive and Critical Care Societies 21:e52-e106
28. Sun X, Zhou R, Lei Y, Hu J, Li X (2020) The ligand-gated ion channel P2X7 receptor mediates NLRP3/caspase-1-mediated pyroptosis in cerebral cortical neurons of juvenile rats with sepsis.Brain Res1748
29. Mazeraud A, Righy C, Bouchereau E, Benghanem S, Bozza F, Sharshar T (2020) Septic-Associated Encephalopathy: a Comprehensive Review. Neurotherapeutics: the journal of the American Society for Experimental NeuroTherapeutics 17:392–403
30. Asada M, Hayashi H, Takagi N (2022) Possible Involvement of DNA Methylation and Protective Effect of Zebularine on Neuronal Cell Death after Glutamate Excitotoxity. Biol Pharm Bull 45:770–779
31. Gonzalez J, Jurado-Coronel J, Ávila M, Sabogal A, Capani F, Barreto G (2015) NMDARs in neurological diseases: a potential therapeutic target. Int J Neurosci 125:315–327
32. Kim B, Ahn J, Kim D, Lee T, Kim Y, Shin M, Cho J, Kim Y, Park J, Kang I, Lee J, Won M (2021) Transient forebrain ischemia under hyperthermic condition accelerates memory impairment and neuronal death in the gerbil hippocampus by increasing NMDAR1 expression. Molecular medicine reports 23
33. Schmutzhard J, Glueckert R, Pritz C, Blumer MJF, Bitsche M, Lackner P, Fille M, Riechelmann H, Harkamp M, Sitthisak T, Schrott-Fischer A (2013) Sepsis otopathy: experimental sepsis leads to significant hearing impairment due to apoptosis and glutamate excitotoxicity in murine cochlea. Dis Model Mech 6:745–754

34. Dal Pizzol F, Zhang S, Wang X, Ai S, Ouyang W, Le Y, Tong J (2017) Sepsis-induced selective loss of NMDA receptors modulates hippocampal neuropathology in surviving septic mice. PLoS ONE 12:e0188273
35. Karki P, Lee E, Aschner M (2013) Manganese neurotoxicity: a focus on glutamate transporters. Annals of occupational and environmental medicine 25:4
36. Rimmele T, Rosenberg P (2016) GLT-1: The elusive presynaptic glutamate transporter. Neurochem Int 98:19–28
37. Tanaka K, Watase K, Manabe T, Yamada K, Watanabe M, Takahashi K, Iwama H, Nishikawa T, Ichihara N, Kikuchi T, Okuyama S, Kawashima N, Hori S, Takimoto M, Wada K (1997) Epilepsy and exacerbation of brain injury in mice lacking the glutamate transporter GLT-1. Sci (New York NY) 276:1699–1702
38. Mochida S (2021) Stable and Flexible Synaptic Transmission Controlled by the Active Zone Protein Interactions.Int J Mol Sci22
39. Chamma I, Sainlos M, Thoumine O (2020) Biophysical mechanisms underlying the membrane trafficking of synaptic adhesion molecules. Neuropharmacology 169:107555
40. Quade B, Camacho M, Zhao X, Orlando M, Trimbuch T, Xu J, Li W, Nicastro D, Rosenmund C, Rizo J (2019) Membrane bridging by Munc13-1 is crucial for neurotransmitter release. eLife 8
41. Wierda KD, Toonen RF, de Wit H, Brussaard AB, Verhage M (2007) Interdependence of PKC-dependent and PKC-independent pathways for presynaptic plasticity. Neuron 54:275–290
42. Toklu HZ, Uysal MK, Kabasakal L, Sirvanci S, Ercan F, Kaya M (2009) The Effects of Riluzole on Neurological, Brain Biochemical, and Histological Changes in Early and Late Term of Sepsis in Rats. J Surg Res 152:238–248
43. Lazarevic V, Yang Y, Ivanova D, Fejtova A, Svenningsson P (2018) Riluzole attenuates the efficacy of glutamatergic transmission by interfering with the size of the readily releasable neurotransmitter pool. Neuropharmacology 143:38–48
44. Kasula R, Chai YJ, Bademosi AT, Harper CB, Gormal RS, Morrow IC, Hosy E, Collins BM, Choquet D, Papadopulos A, Meunier FA (2016) The Munc18-1 domain 3a hinge-loop controls syntaxin-1A nanodomain assembly and engagement with the SNARE complex during secretory vesicle priming. J Cell Biol 214:847–858
45. Gil-Pisa I, Munarriz-Cuezva E, Ramos-Miguel A, Urigüen L, Meana JJ, García-Sevilla JA (2011) Regulation of munc18-1 and syntaxin-1A interactive partners in schizophrenia prefrontal cortex: down-regulation of munc18-1a isoform and 75 kDa SNARE complex after antipsychotic treatment. Int J Neuropsychopharmacol 15:573–588
46. Das P, Chopra M, Sharma AC (2008) Upregulation of myocardial syntaxin1A is associated with an early stage of polymicrobial sepsis. Mol Cell Biochem 323:61–68
47. Han GA, Malintan NT, Saw NMN, Li L, Han L, Meunier FA, Collins BM, Sugita S, Glick B (2011) Munc18-1 domain-1 controls vesicle docking and secretion by interacting with syntaxin-1 and chaperoning it to the plasma membrane. Mol Biol Cell 22:4134–4149
48. Egbujo CN, Sinclair D, Hahn C-G (2016) Dysregulations of Synaptic Vesicle Trafficking in Schizophrenia. Curr Psychiatry Rep 18:77
49. Schwalm MT, Pasquali M, Miguel SP, dos Santos JPA, Vuolo F, Comim CM, Petronilho F, Quevedo J, Gelain DP, Moreira JCF, Ritter C, Dal-Pizzol F (2013) Acute Brain Inflammation and Oxidative Damage Are Related to Long-Term Cognitive Deficits and Markers of Neurodegeneration in Sepsis-Survivor Rats. Mol Neurobiol 49:380–385
50. Catalão CHR, Santos-Junior NN, da Costa LHA, Souza AO, Cárnio EC, Sebollela A, Alberici LC, Rocha MJA (2020) Simvastatin Prevents Long-Term Cognitive Deficits in Sepsis Survivor Rats by Reducing Neuroinflammation and Neurodegeneration. Neurotox Res 38:871–886